Dielectrophoretic nanoparticle injector for photonic manipulator systems

Jaykob Maser, Joshua Rovey

Jaykob Maser, Joshua Rovey, "Dielectrophoretic nanoparticle injector for photonic manipulator systems," Proc. SPIE 10982, Micro- and Nanotechnology Sensors, Systems, and Applications XI, 1098238 (13 May 2019); doi: 10.1117/12.2518920

SPIE.

Event: SPIE Defense + Commercial Sensing, 2019, Baltimore, Maryland, United States

Dielectrophoretic Nanoparticle Injector for Photonic Manipulator Systems

Jaykob Maser
Missouri University of Science and Technology
Rolla, Missouri

Joshua Rovey
University of Illinois at Urbana-Champaign
Urbana, Illinois

ABSTRACT

We describe the concept of a dielectrophoretic nanoparticle injector and its use in a plasmonic/photonic-based nanoparticle manipulation system. Motion is achieved by generating an electrostatic, non-uniform field between two tilted plates and applying the corresponding dielectrophoretic force to net-neutral nanoparticles.

Keywords—dielectrophoresis, nanoparticles, photonics

1 INTRODUCTION

The manipulation of micro/nanoparticles of solid or aqueous material by way of gradient electromagnetic fields is used extensively in the fields of photonics and microfluidics. Nanoparticle manipulation and acceleration enabled by localized surface plasmon resonance is well-known and originally coined as "plasmon nano-optical tweezers."[1] The plasmon-generated forces have been demonstrated to optically trap particles beyond the diffraction limit.[2] An asymmetric, V-groove type structure was developed by Shalin and Sukhov in 2012 [3] for the one dimensional acceleration and ejection of nanoparticles in a method described as a nanocannon. They propose that ejection of nanoparticles from the V-grooves will occur due to the gradient force of the *E*-field in the grooves and a negative real part of the polarizability of the nanoparticles. Liquid microflows and pico/nanoliter droplets have been manipulated for siphoning[4], separation/mixing[5] in chemical or biological experiments, and transport applications[6]. Liquid tendrils have been guided from a droplet along wall-less straight[7] and curved[8] virtual microchannels enabling enhanced flexibility for the aforementioned transport techniques. Additional nanoparticle acceleration schemes using plasmon generated gradient force fields have been studied for applications in nanosatellite propulsion systems[9-11]. We study a dielectrophoretic tilted plate reservoir that acts as a mass storage device for nanoparticles or microliter quantities of liquids and would enable variable injection of the stored material into manipulation/acceleration schemes such as those mentioned above.

2 DIELECTROPHORETIC INJECTOR

2.1 Theory of dielectrophoresis

Dielectrophoresis occurs when a net-neutral particle is placed in a non-uniform electric field. The electric field polarizes the particle and the polarized particle then feels a force due to the gradient in the magnitude of the field (Figure 1). The direction of the force depends on the difference between the permittivity of the particle and that of the surrounding medium. The dielectrophoretic (DEP) force is utilized in a variety of research fields but most commonly in microfluidics and biomedical applications[12]. Its effectiveness in these areas is due, in part, to its ability to separate particles according to their polarizability and/or size. We desire to make use of its ability to precisely control the motion and flow of a concentration of net-neutral nanoparticles.

Micro- and Nanotechnology Sensors, Systems, and Applications XI, edited by Thomas George, M. Saif Islam, Proc. of SPIE Vol. 10982, 1098238 · © 2019 SPIE
CCC code: 0277-786X/19/$18 · doi: 10.1117/12.2518920

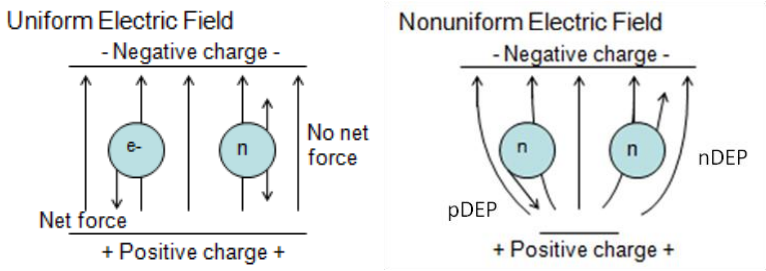

Figure 1: Particle Motion in Uniform and Non-uniform Electric Fields

Research has shown that dielectrophoresis can be used to continuously pump particle-laden microfluidic flows through virtual (wall-less) channels using microstructured electrodes in a variety of configurations[6]. Research has also shown that dielectrophoresis can filter particles from a stream of gas; expanding the usability of the DEP mechanism[13]. Further progress in this field has demonstrated that particulate matter can be separated by use of dielectrophoresis in a vacuum environment, known as vacuum dielectrophoresis[14]. Vacuum dielectrophoresis eliminates certain interactions due to the particles moving in a medium/fluid, making the DEP force the only interaction with the particles in the plane perpendicular to the force of gravity.

The DEP-induced motion depends on the dielectric properties of the particles and the surrounding medium. Specifically, it depends on the effective polarization of the suspended particles. If the polarizability of a net-neutral nanoparticle is greater than the polarizability of the surrounding medium, then the nanoparticle will be pushed toward the stronger region of the electric field (pDEP) and vice-versa (nDEP) if the medium has higher polarizability. Equations (1) and (2) define the DEP force acting on a particle.

$$\vec{F}_{DEP} = 2\pi R^3 \varepsilon_m k \nabla\left(\left|\vec{E}\right|\right)^2 \tag{1}$$

$$k = \frac{\epsilon_p - \epsilon_m}{\epsilon_p + 2\epsilon_m} \tag{2}$$

R is the radius of the particle. ε_m is the permittivity of the surrounding medium in which the particles are suspended. k is the Clausius-Mossotti factor, defined in Equation (2), that relates the permittivity of the particle and medium and is positive when the particle permittivity is greater than the medium permittivity. $\vec{E}$ is the electric field. From these equations we see that the DEP force is proportional to the cube of the radius of the suspended particles as well as the gradient of the magnitude of the electric field.

2.2 Dielectrophoretic injector design

The DEP force can be used to inject nanoparticles into a photonic particle manipulator. As described above, the DEP force is active in the presence of a non-uniform electric field. It acts on net-neutral particles along the direction of the gradient of the non-uniform field. Therefore, to harness the DEP force and use it to propel nanoparticles into particle manipulating platforms, we must design an electric field that is non-uniform and whose gradient tends to lie along a single direction. We investigate here a wedge-shaped prism, whose 2-D cross section is a simple tilted plate capacitor. This geometry creates a steady, non-uniform electric field when supplied with a DC voltage and the electric field can be easily solved analytically in 2-dimensions using the following equation derived from Coulomb's Law for the electric field due to a distributed charge.

$$\vec{E}(\vec{r}) = \frac{1}{4\pi\varepsilon_0}\int \rho(\vec{r}\,')\frac{\vec{r}-\vec{r}\,'}{|\vec{r}-\vec{r}\,'|^3}d^3\vec{r}\,' \tag{3}$$

For 2-dimensions, let the charge density $\rho(\vec{r}') \rightarrow \lambda(\vec{r}') = Q/L$ where Q is the charge on the plate and L is its length. With this reduction and the definitions in Equations **(**4**)**, **(**5**)** and **(**6**)** that give the location of a test point and shape of the surfaces, we can define the total electric field between the surfaces as the sum of the electric fields produced by each surface, Equation (7).

$$\vec{r} = y_0\hat{j} + z_0\hat{k} \tag{4}$$

$$\vec{r}_L{}' = y'\hat{j} + (my' - h)\hat{k} \tag{5}$$

$$\vec{r}_U{}' = y'\hat{j} + (h - my')\hat{k} \tag{6}$$

$$\vec{E}(\vec{r}) = \overrightarrow{E_U}(\vec{r}(y,z)) + \overrightarrow{E_L}(\vec{r}(y,z)) \tag{7}$$

Figure 2 illustrates the variables contained in Equations (4) - (6).

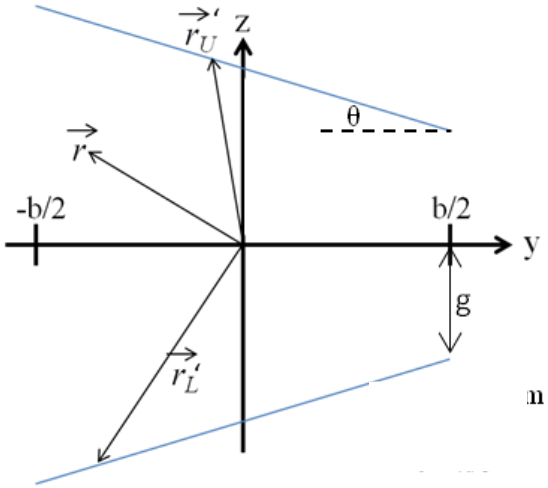

Figure 2: Visual Definitions of Variables in Equations **(**4**)**, **(**5**)**, and **(**6**)**. $b = 50\ \mu m, g = 7\ \mu m, \theta =$ variable.

The tilted plate capacitor cross-section is shown in Figure 3, where the red lines show the silhouette of the injector, and the design is such that the particles will start in the injector (injector doubles as a storage tank) and then exit to the manipulation platform on the right. The upper and lower surfaces of the injector (red lines in the image) are electrically separated and a potential difference is maintained across them in order to produce the desired electric field. A dielectric, rectangular guide-sleeve (solid blue lines) is inserted along the axis of the injector between the charged surfaces with separation distance equal to the opening width, $2g$, of the injector exit. The dielectric guide sleeve keeps the particles away from the conducting plates where, in close proximity to the plates, the gradient of the electric field pointing toward the plate would act to trap them in pDEP.

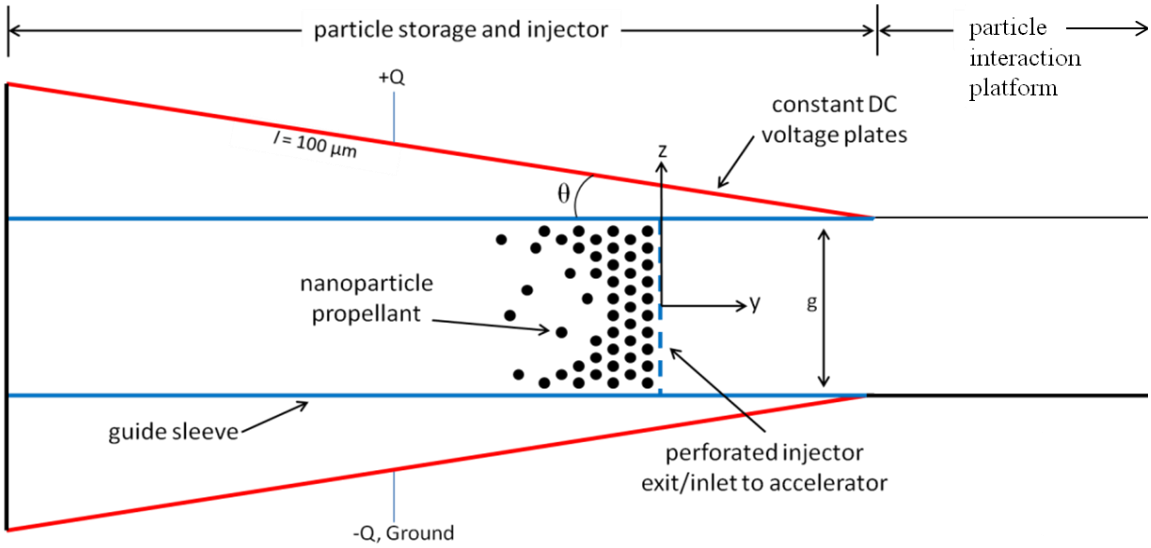

Figure 3: Geometry of Tilted Plate Nanoparticle Injector

Summing the electric fields due to the upper and lower plates allows the conversion of Equation (3) to Equation (7) with $\overrightarrow{E_L}$, the electric field produced by the lower plate, defined by Equation (8) and $\overrightarrow{E_U}$, the electric field produced by the upper plate, defined in Equation (9).

$$\overrightarrow{E_L}\left(\vec{r}(y,z)\right) = \frac{Q}{4\pi b\varepsilon_0}\int_{-b/2}^{b/2} \frac{(y_0 - y')\hat{j} + (z_0 - my' + h)\hat{k}}{((y_0 - y')^2 + (z_0 - my' + h)^2)^{3/2}}\,dy' \tag{8}$$

$$\overrightarrow{E_U}\left(\vec{r}(y,z)\right) = \frac{-Q}{4\pi b\varepsilon_0}\int_{-b/2}^{b/2} \frac{(y_0 - y')\hat{j} + (z_0 + my' - h)\hat{k}}{((y_0 - y')^2 + (z_0 + my' - h)^2)^{3/2}}\,dy' \tag{9}$$

The electric field produced by this setup is plotted in Figure 4 (a) for plate angle $\theta = 0.0°$ and Figure 4 (b) for $\theta = 25°$. For validation, the $\theta = 0°$ case is compared to the electric field produced by a parallel plate capacitor, which assumes infinite electrodes, $E_{cap} = V/d$. E is the electric field, V the electric potential difference between the two plates, and d the separation distance between the two plates. With $V = 2.0\,V$ and $d = 14\,\mu m$, $E_{cap} \cong 142.9\,kV/m$. Let $V = 2.0\,V$ and $d = 14 \pm 0.16\,\mu m$ for the analytical model solution with finite electrodes. The minor difference in plate separation values is an intentional offset for the analytical solution because the electric field derived from Coulomb's law is proportional to $1/r^2$, which means that as d approaches $14\,\mu m$, the distance to the second plate approaches zero and the electric field contribution goes to infinity. The electric field produced by the plates in the analytical solution, at the point $y = -25\,\mu m, z \cong 7\,\mu m$ where the field is max, is $E_{analytical} \cong 143.5\,kV/m$. The percent error between the finite plate analytical and infinite plate parallel capacitor solutions is 0.42 % .The electric field distribution in Figure 4 (b) for the $\theta = 25°$ plate angle is steady and non-uniform, increasing in strength from left to right. The solid, black, diagonal lines represent the edges, or silhouette, of the wedge-shaped injector while the short vector lines indicate the electric field produced between the electrodes. Along the centerline ($z = 0$), one can see that the electric field lines increase in strength with increasing y-position. These properties are plotted in Figure 5. We have disregarded the configuration of the electric field outside of the particle injection structure because it has no effect on the motion of the particles and is assumed to be shielded.

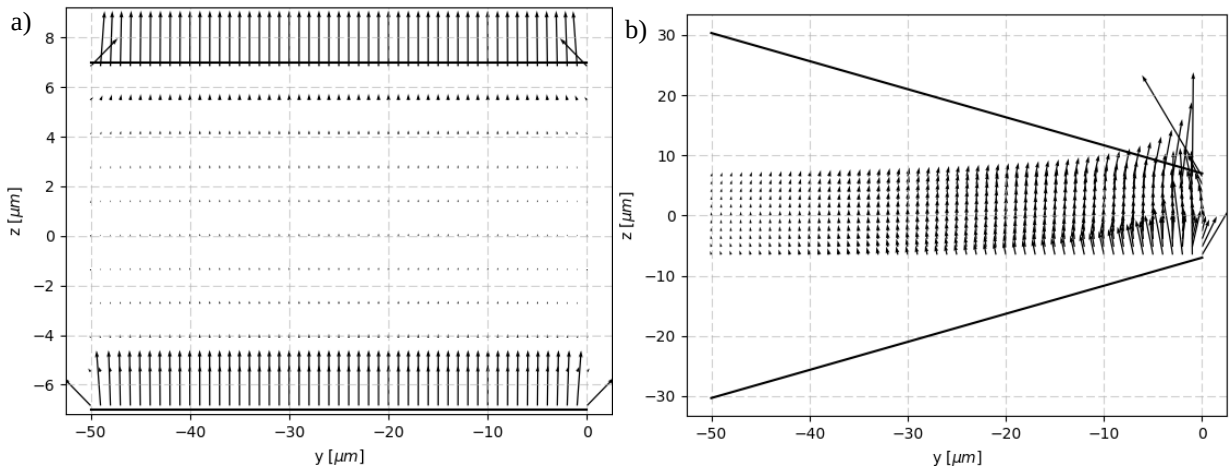

Figure 4: Electric Field Vectors between Electrodes with Plate Angle (a) $\theta = 0°$ and (b) $\theta = 25°$

In Figure 5, contours of the electric field along the centerline and 3 μm above and below the centerline are plotted versus the distance along the axis of the injector. E_z and E_y are the electric field components in the z- and y-directions, respectively. The dotted red line in Figure 5 shows that the y-component of the electric field along the axis of the injector is zero for the whole axis. This is expected because as the electric field lines curve from one electrode to the other, they are perpendicular to the centerline axis of the injector at the centerline. The off-axis y-components of the electric field contour show that there is a transition region where the electric field reverses direction inside the injector (yellow dotted line and black dot-dash line at $y \approx -4.5\ \mu m$). This phenomenon poses a potential problem because the gradient of the electric field also changes sign (observe the slope of the yellow dotted line and black dot-dashed line for $-15\ \mu m < y < -5\ \mu m$) which could indicate a trapping region for the nanoparticles if pDEP is utilized. The transition region is also visible in the slope of the off-axis contours of the z-component of the electric field (blue solid, red dot-dot, and cyan dash lines for $-7.5\ \mu m < y < -2.5\ \mu m$).

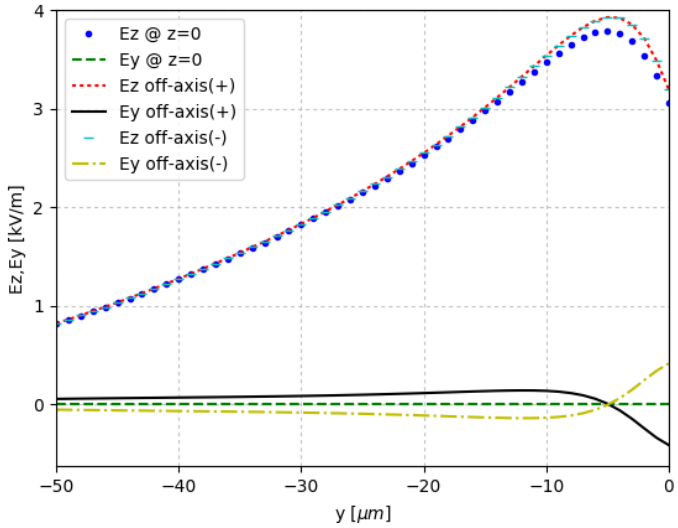

Figure 5: Axial and Transverse Electric Field Line Contours between Angled Electrodes

As stated previously, the DEP force is calculated from the gradient of the magnitude of the electric field. Figure 6 contains contour plots of the gradient in the (a) y-direction and (b) z-direction (the signed natural logarithm is used to create a higher contrast visual of the data) and Figure 6 (c) is a line contour of the characteristic force along the axis of

the injector. The characteristic force is the DEP force divided by the cubed radius of the nanoparticles such that Equation (1) becomes Equation (10) with units of N/m^3.

$$\frac{\vec{F}_{DEP}}{R^3} = 2\pi\varepsilon_m k\nabla\left(\left|\vec{E}\right|\right)^2 \tag{10}$$

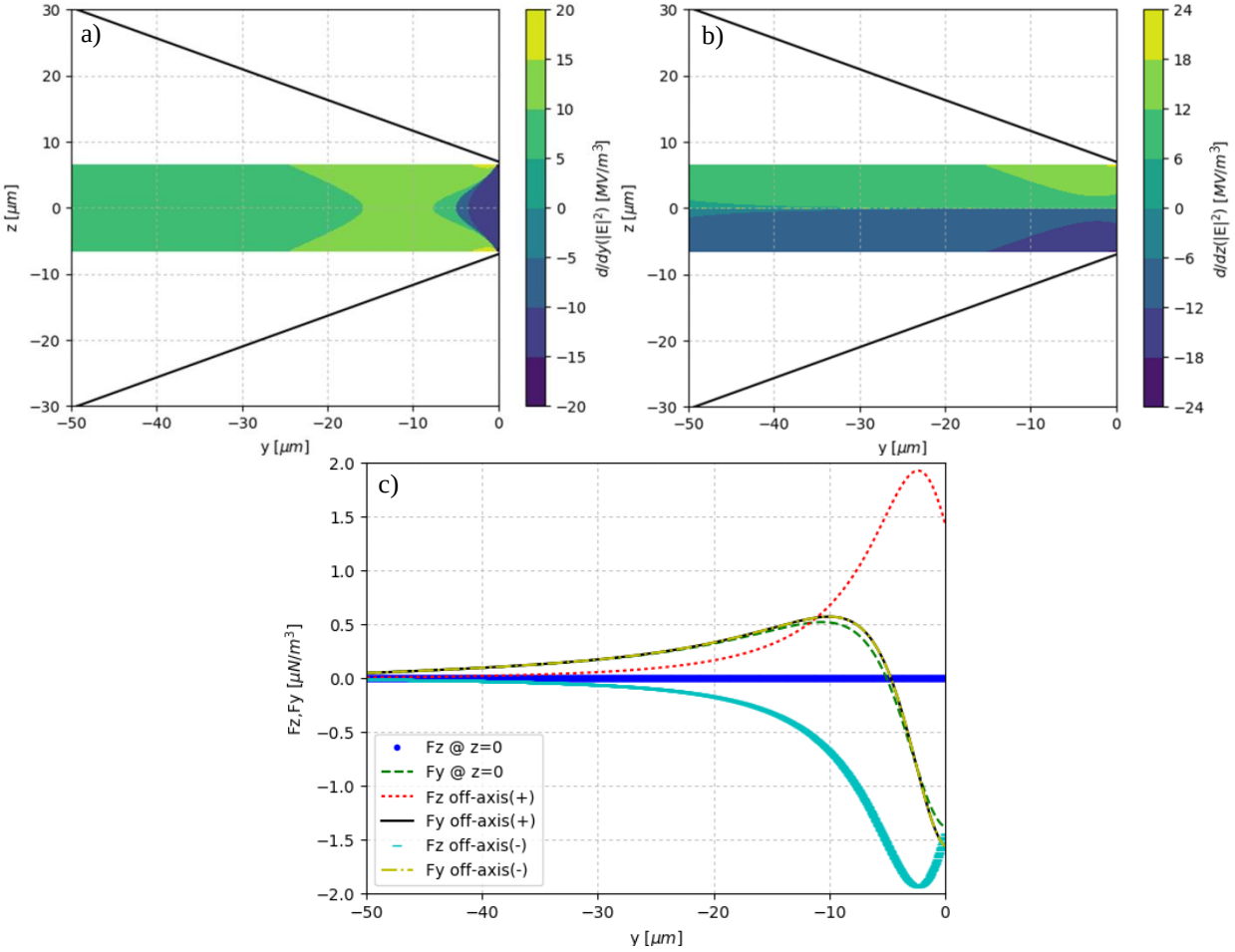

Figure 6: (a) Y-Gradient of the Magnitude of the Electric Field, (b) Z-Gradient of the Magnitude of the Electric Field, (c) DEP Force Profile along Axis of Angled Electrodes (at the centerline and $\pm 3\ \mu m$ off the centerline) (plate angle 25°)

The force in the y- and z-directions at three values of $z = 0, 3, -3\ \mu m$ are plotted in Figure 6 (c). F_y for all three z values begins positive and then goes negative near $y \cong -5\ \mu m$. Studying the y-gradient of the electric field magnitude indicates that this behavior is expected because following the gradient from left to right in Figure 6 (a), along the axis, one sees that the gradient begins positive, increases, then decreases and goes negative. The force is proportional to this profile as shown in Equation (10). Contrary to F_y, F_z behaves differently for each z value. When $z = 0\ \mu m$ the force in the z-direction is also zero along the entire axis because the z-gradient of the electric field magnitude crosses an inflection point in this location. When $z = 3\ \mu m$ the z-gradient is positive which shows the electric field increasing toward the electrode as the $1/r^2$ dependence indicates it should. Increasing y position effectively brings the electrode closer to the $z = 3\ \mu m$ line which also follows the $1/r^2$ dependence and we see a corresponding increase in F_z. When $z = -3\ \mu m$, F_z mirrors the behavior of F_z when $z = 3\ \mu m$. The force is negative, pointing along the gradient directed towards the lower electrode.

2.3 Finite Element Analysis

The analytical solution is used to study particle dynamics within the tilted plate injector. COMSOL Multiphysics numerical models were also developed in order to study more complex electrode geometries and electric field structures. The initial geometry used for the numerical models is composed of the tilted, charged plates and the dielectric guide sleeve that restricts the motion of the nanoparticles. Figure 7 shows a contour plot of the magnitude of the electric field between the two tilted plates. The field structure supports our understanding of the analytically obtained results in Figure 4 (b) wherein the field strength increases towards the narrow end of the injector and near the electrodes. The electric field magnitude at location

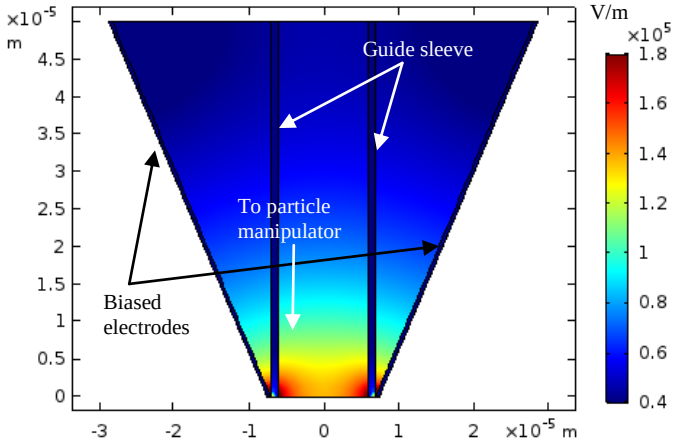

Figure 7: COMSOL Multiphysics Model of Electric Field Magnitude in Tilted Plate Injector (injector in this image is rotated 90° clockwise and is pictured with the hollow dielectric guide sleeve)

The perforated exit/inlet membrane that guides the injection of the nanoparticles, indicated in Figure 3, was also included in COMSOL models to determine its affect on the electric field structure. Our design calls for a metallic membrane that acts as a floating potential and shields part of the dielectric guide sleeve from the applied electric field at the location where the electric field gradient changes direction as indicated in Figure 5. A concern we have with this membrane is that the electric field will reduce to zero too quickly at the location of the perforations and the resultant gradient will create a strong DEP force acting against the motion of the nanoparticles. Figure 8 shows the force field contours for the tilted plate injector with a perforated metallic membrane acting as a floating electrical ground. The perforations in the membrane are perpendicular to the axis of the injector and act as a gate through which the nanoparticles pass. From this contour plot, we see that the presence of the metallic membrane does create force acting against the motion of the particles (the red/orange/yellow bulge in the center of the plot, focused at the perforated membrane).

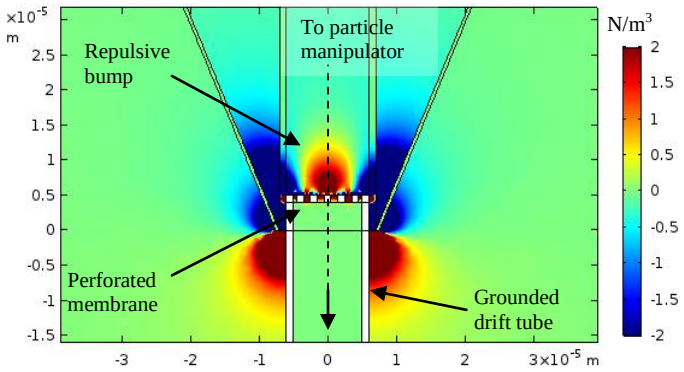

Figure 8: COMSOL Multiphysics Model of Force Field in Tilted Plate Injector with Dielectric Guide Sleeve and Metallic Perforated Membrane as Floating Ground

The DEP force depends on the relative polarizability of the nanoparticles to the surrounding medium which is vacuum, as stated earlier. This means that the dielectric constant of the nanoparticles is greater than the dielectric constant of the medium, vacuum, and the DEP force takes on the sign of the gradient of the electric field magnitude. If the medium had a dielectric constant that was greater than that of the nanoparticles then the DEP force would be the negative of the sign of the gradient in the electric field magnitude. Therefore, a possible solution to the strong negating force issue that the perforated membrane poses is to suspend the nanoparticles in a liquid such as water rather than vacuum. The resulting force field contour of the tilted plate injector that is filled with water and has a dielectric guide sleeve and a metallic perforated membrane is plotted in Figure 9. This contour shows that the repulsive hump seen in Figure 8 now becomes an accelerating ramp that assists the motion of the nanoparticles.

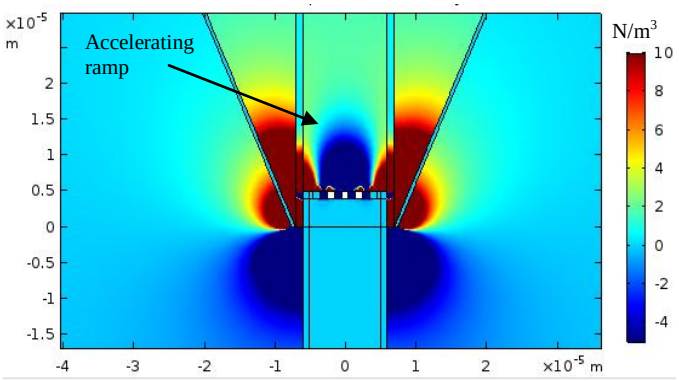

Figure 9: COMSOL Multiphysics Model of Force Field in Tilted Plate Injector with Water as the Suspension Material, a Dielectric Guide Sleeve, and a Metallic Perforated Membrane as Floating Ground

3 CONCLUSION

We have investigated a dielectrophoretic nanoparticle injection mechanism that can couple with a photonic acceleration/manipulation platform. The injector consists of tilted plates that are electrically isolated and charged to maintain a steady, nonuniform electric field across a vacuum or liquid-filled gap. We have analytically and numerically modeled the electric field and dielectrophoretic force within the space between the tilted plates. Finally, we conclude that the nanoparticles must be suspended in a medium with dielectric constant greater than that of the nanoparticles so that the metallic membrane acting as a floating potential and gate will aid their motion and not hinder it.

4 REFERENCES

[1] Juan, M. L., Righini, M. & Quidant, R. "Plasmon nano-optical tweezers," Nat. Photonics **5**, 349-356 (2011).

[2] Shoji, T. & Tsuboi, Y. "Plasmonic optical tweezers toward molecular manipulation: tailoring plasmonic nanostructure, light source, and resonant trapping," J. Phys. Chem. Lett. **5**, 2957-2967 (2014).

[3] Shalin, A. & Sukhov, S. "Plasmonic nanostructures as accelerators for nanoparticles: optical nanocannon," Plasmonics **8**, 625-629 (2012).

[4] Kaler, K. V. I. S., Prakash, R. & Chugh, D. "Liquid dielectrophoresis and surface microfuidics," Biomicrofluidics **4** (2010).

[5] Park, S.-Y., Kalim, S., Callahan, C., Teitell, M. & Chiou, E. "A light-induced dielectrophoretic droplet manipulation platform," Lab on a chip **9**, 3228-3235 (2009).

[6] Fan, S. K., Chen, W. J., Lin, T. H., Wang, T. T. & Lin, Y. C. "Reconfigurable liquid pumping in electric-field-defined virtual microchannels by dielectrophoresis," Lab on a chip **9**, 1590-1595, doi:10.1039/b900790c (2009).

[7] Wang, K.-L., Jones, T. B. & Raisanen, A. "Dynamic control of DEP actuation and droplet dispensing," J. Micromech. Microeng. **17**, 76-80 (2007).

[8] Gunji, M., Jones, T. B. & Washizu, M. "Dielectrophoretic microfluidic devices."

[9] Maser, J. N., Rovey, J. L., Yang, X., Li, L., Deng, H. in *54th Aerospace Sciences Meeting.*AIAA-2016-0696 edn.
[10] Maser, J. N., Li, L., Deng, H., Yang, X. & Rovey, J. L. "Transmission spectrum of asymmetric nanostructures for plasmonic space propulsion," J. Spacecraft. Rockets **53**, 998-1000 (2016).
[11] Rovey, J. L., Friz, P. D., Hu, C., Glascock, M. S. & Yang, X. "Plasmonic force space propulsion," J. Spacecraft Rockets **52**, 1163-1168 (2015).
[12] Pethig, R. "Review article—dielectrophoresis: status of the theory, technology, and applications," Biomicrofluidics **4**, 022811, doi:10.1063/1.3456626 (2010).
[13] Duff, J. D. "Dielectrophoretic precipitation of airborne particles," M. Eng. thesis, University of Louisville, (2013).
[14] Sagar, A. & Rose, R. in *26th Aerospace Sciences Meeting Aerospace Sciences Meetings* (American Institute of Aeronautics and Astronautics, 1988).